Automotive Experiences
Vol. 7 No. 2 (2024) pp. 207-223
p-ISSN: 2615-6202 e-ISSN: 2615-6636

Research Paper

# Evaluation the New Hydro-Pneumatic Damper for Passenger Car using LQR, PID and H-infinity Control Strategies

**M. Rabie Abd - Elwahab[1], Ahmad O. Moaaz[2], Waleed Fekry Faris[3], Nouby M. Ghazaly[4,5], and Mostafa M. Makrahy[1]**

[1]Automotive and Tractor Eng. Dept., College of Engineering, Minia University, 61519, El-Minia, Egypt
[2]Mechanical Engineering Department, Faculty of Engineering, Beni-suef University, 62521, Beni-suef, Egypt
[3]Department of Mechanical Engineering, College of Engineering, International Islamic University Malaysia, Kuala Lumpur 53100, Malaysia
[4]Mechanical Eng. Dept., Faculty of Engineering, South Valley University, Qena-83523, Egypt
[5]Technical College, Imam Ja'afar Al-Sadiq University, 1983969411, Baghdad, Iraq

nouby.ghazaly@eng.svu.edu.eg

https://doi.org/10.31603/ae.10796

Published by Automotive Laboratory of Universitas Muhammadiyah Magelang

*Article Info*
*Submitted:* 23/03/2024
*Revised:* 10/05/2024
*Accepted:* 04/06/2024
*Online first:* 04/08/2024

## Abstract

In this study, a mathematical model of a new hydro-pneumatic damper consists of a double-acting cylinder, two oil chambers, a damping valve, and an accumulator is developed to assess its response to vertical vibrations in a passenger car. The main idea of the new damper aim to make that the damping coefficient in compression differ than that in rebound which achieve more stability specially during cornering. The damping coefficient difference in compression and rebound can be achieved due to the presence of accumulator. Both passive and active hydro-pneumatic suspension systems with the new damper employing different control strategies such as LQR, PID, and H-infinity control, are employed to assess the effectiveness of the suspension system. The investigation focuses on vertical acceleration, pitch acceleration, suspension deflection, and dynamic tire load. The half-car model is simulated using MATLAB/Simulink, and the results for both active and passive hydro-pneumatic suspensions are analyzed in terms of frequency, time, and power spectral density responses. The findings reveal that the active suspension system with H-infinity control demonstrates an 81% improvement in body acceleration and a 92% improvement in pitch acceleration (angular acceleration) compared to the passive hydro-pneumatic suspension which improve the stability of the vehicle during cornering. Similarly, the implementation of LQR-controlled suspension enhances body acceleration and step acceleration by approximately 40% and 57%, respectively, compared to the passive hydro-pneumatic suspension. Moreover, when compared to the passive hydro-pneumatic suspension, the PID-controlled active hydro-pneumatic suspension exhibits a 64% improvement in step acceleration and a 44% improvement in body acceleration.

**Keywords:** PID Control; LQR Control; H-infinity Control; Hydro-pneumatic suspension; Suspension performance; Vehicle stability; Ride comfort

## 1. Introduction

In general, passenger comfort is an important parameter in vehicle design and production. The suspension system has many functions, including supporting the vehicle structure and absorbing vibrations conveyed to the vehicle body from the road. These vibrations result from unevenness in the roadway, aerodynamic forces, and uneven wheels. Driving comfort means that bumps or shocks are not transferred to the passenger or are minimal from the road surface. Ride comfort is indicated by acceleration, whereas stability is assessed by suspension deflection as well as tire load. Ride comfort is maximized when the sprung masses accelerate as little as possible, which is a measure of passenger comfort [1], [2].

The hydro-pneumatic suspension system application has become widespread, and the influence factors that affect ride performance have become significant [3], [4]. A lot of research has been done in the field of optimization to improve driving comfort. Many optimization methods are used, including gradient-based methods, evolutionary operations of the rotating square (ROVOP), genetic algorithms, and sequential research methods [5]. Although the various multipurpose optimization methods represent one direction in chassis design, the study and examination of ride comfort represent an important factor [6]. Theoretical research has demonstrated that a suspension system for a vehicle that has a lower spring mass and a natural frequency can improve comfort while driving [7], [8].

The suspension systems used in the field of the vehicle industry can be divided into three main categories: passive, semi-active, and active suspension. The passive elements (spring and shock absorber) are used to design the passive suspension system; these passive elements are selected based on the vehicle design for the best performance or greater comfort [9], [10]. Active suspensions are feedback-based control systems that utilize signals representing system variables to regulate the actuators, either instead of or in conjunction with passive components. The necessary forces to power the different components of active suspension such as potentiometers, force transducers, and actuators, as well as conditioning and amplification devices are provided by external energy [11]–[14].

The semi-active damper system was first introduced at the start of the 1970s. A semi-active system offers a variable damping force, such as an electro-rheological damper (ER) or a magneto-rheological damper (MR), that applies different electric or magnetic fields to create a variable damping coefficient [15], [16]. The main advantage of the active suspension system over the semi-active suspension system is that it offers better driving performance. The disadvantages of active suspension are a large external power source, greater complexity and cost, and lower reliability. Compared to passive suspension, semi-active suspension offers good driving behavior, is economical, safe, and does not require more powerful actuators or a large power supply. The semi-active suspension system combines the adaptability of an active control system with the dependability of a passive suspension system. As a result, research on semi-active suspension systems has expanded quickly [17], [18].

The control methods are often used with semi-active shock absorbers since they are relatively simple. To improve performance in different vehicles and road conditions, numerous control techniques for the semi-active shock absorber have been suggested. Skyhook Control (SKH) has been used successfully in semi-active suspensions. Skyhook controls are simple to use and don't require much information about the vehicle's condition. It's required to provide a virtual damper between the vehicle's body and the imaginary sky [19]. Modeling the chassis model with optimal control with the suggestion of an optimal microcomputer model [20]. The goal of the best control strategy and optimization method was to improve the semi-active suspension's performance. A bilinear regulator considerably raises the running quality [21]. An optimal controlling law was built and compared to different semi-active control laws using a time-varying feedback gain matrix technique [22]. A new concept of semi-active control has been proposed, known as Ground Hook Control (GRD). The suggested control inputs were the sprung mass speed and the feedback about the tire deflection [23]. The basic concept of the earth hook was proposed in an attempt to minimize the criteria for road damage and to maintain good comfort [24]. A new adaptive damping strategy based on constant damping options has been proposed [25]. The semi-active two-state damper controlled using hybrid control was used in a quarter cars and compared to a hybrid control damper with a fixed damping coefficient [26]. Investigation into the performance of a hybrid control system using a magneto-rheological (MR) damper in a quarter-car model reveals that the method can benefit both sprung and unsprung masses [27]. Additionally, a semi-active hydro-pneumatic suspension (HP) model and a suspension observer based on the Kaman Unscented (UKF) filter theory were designed and proposed for the hybrid control algorithm [28], [29].

In driving dynamics, a single suspension is controlled by the existing quarter-car model, which is often used to control the performance of a suspension adjuster. The two-degree-of-freedom model (quarter-car model) is expanded to four degrees of freedom in the four-degree-of-freedom model (half-car model), requiring the use of four differential equations. Discoverable elements have also been added during the expansion. With the 2-DOF model, it is possible to analyze only the bending of the wheel and the bending of the suspended mass; with the 4-DOF model, on the other hand, the angle of inclination of the suspended mass (body) and the bending of the added wheel can be analyzed in the existing items.

In this investigation, a 4-degree-of-freedom (4-DOF) half-car model undergoes the influence of a random road input. Both passive and active hydro-pneumatic suspensions, integrated with diverse controller systems—namely, LQR, PID, and H-infinity control—are employed to regulate the damping force within the suspension system. The simulation is conducted utilizing Matlab/Simulation software, offering an analysis of the effectiveness of passive hydro-pneumatic and active systems when employing LQR, PID, and H-infinity control methodologies. A simulation model is used to compare and evaluate the dynamic behavior of both active suspension and passive suspension systems for a half-car suspension model with LQR, PID, and H-infinity control. To evaluate body shift, front/rear shift, and pitch angle for varying road conditions, a half-car model with four degrees of freedom is employed.

## 2. New Passive Hydro-Pneumatic Suspension System

In this study, a new hydro-pneumatic suspension is used to examine its influence on ride comfort (braking and acceleration) using a half-automobile model. **Figure 1**, displays a hydro-pneumatic suspension system that consists of a double-acting cylinder, two oil chambers, a damping valve, and an accumulator. The two chambers are connected by a flow control valve, and the accumulator is also connected to the chamber through a damping valve. The main idea of the new damper aim to make that the damping coefficient in compression differ than that in rebound which achieve more stability specially during cornering. The damping coefficient difference in compression and rebound can be achieved due to the presence of accumulator. The damping coefficient difference in compression and rebound improve the stability of the vehicle. The main operating principle of hydro-pneumatic suspension with the new damper can be described as follows: When the piston ascends, oil from the cylinder chamber is directed to the accumulator via the damping valve. Simultaneously, the oil passes through the damping valve into the second chamber, pressurizing the gas within the accumulator. The flow of oil through the damper valve orifice results in energy consumption, effectively rapidly dampening vibrations. Concurrently, some energy is stored in the accumulator. As the piston descends, oil from the accumulator travels through the damping valve orifice into the chamber, releasing the stored energy from the accumulator. This process reduces the accumulator pressure, allowing the oil to once again and dissipate energy through the damper valve orifice [14]. The stiffness characteristics analysis is [30]:

$$A_P = \frac{\pi}{4} {D_P}^2 \tag{1}$$

Where,

$A_P$ : Cylinder piston area.

$D_P$ : Piston diameter (m).

$$F_s = (P - P_a)A_P \tag{2}$$

Where:

$F_s$ : Gas spring force in the accumulator.

P: Accumulator gas pressure.

$P_a$ : Atmospheric pressure

The accumulator gas is the nitrogen. The nitrogen gas state equation is described as follows [30]:

$$PV^n = P_0 {V_0}^2 = P_j {V_j}^n = C \tag{3}$$

Where,

$P_o$ : The accumulator's initial gas pressure.

$V_o$ : Accumulator initial gas volume.

P: Accumulator instant gas pressure.

V: Accumulator instant gas volume.

$P_j$ : Accumulator gas balance pressure.

$V_j$ : Accumulator gas balance volume.

Considering s as the distance traveled by the piston to reach the static balancing point, we may calculate:

$$S = \frac{V_j - V}{A_P} \tag{4}$$

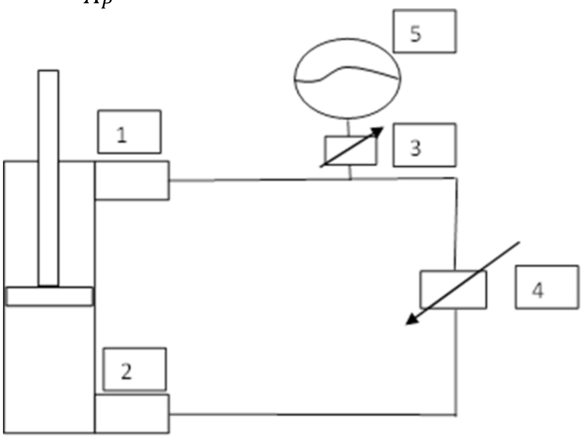


**Figure 1**. Layout of the hydro-pneumatic passive suspension system [14]. (1,2- Oil chambers; 3,4- Damping Valves; 5- Accumulator)

Substitute from Eq. (4) into Eq. (3), thus:

$$F = \frac{P_j {V_j}^n}{\left(V_j - A_P.S\right)^n} A_P \tag{5}$$

According to static balance, we get:

$$P_o V_o = P_j V_j \tag{6}$$

$$\left(P - P_j\right) A_P = mg \tag{7}$$

$$P_j = \frac{mg}{A_h} + P_a \tag{8}$$

$$V_j = \frac{P_o V_o}{\frac{mg}{A_h} + P_a} \tag{9}$$

The gas spring stiffness will be:

$$K_s = \frac{dF_s}{d_s} = A_P \frac{d_p}{d_s} = \frac{n p_o {V_o}^n \mathrm{A_P^n}}{\left(\frac{P_o V_o . A_P}{mg + P_a . A_P} - \mathrm{A_P}.S\right)^{n+1}} \tag{10}$$

When the cylinder is compressed, the oil flows into the valve to the accumulator, and the volume flow rate of the oil is:

$$q_1 = A\dot{x} \tag{11}$$

Where, $A$ is the sectional area of the rodless cavity of the cylinder and $\dot{x}$ is the piston displacement.

The flow equation, according to the throttle hole, will be:

$$q_1 = C_1 A_1 \sqrt{\frac{2\Delta p_1}{\rho}} \tag{12}$$

Where;
$q_1$: Rate of the orifice flow.
$C_1$ : The discharge coefficient.
$A_1$ : The orifice area.
$\Delta p_1$ : The pressure difference between both ends of the hole
$\rho$: The oil density.

The pressure difference $\Delta p_1$ is:

$$\Delta p_1 = p_I - p_{II} \tag{13}$$

The damping force through the throttle valve is:

$$f_1 = \Delta p_1 \times A \tag{14}$$

$$f_1 = \frac{\rho}{2} \frac{A^3 \dot{x}^2}{C_1^2 A_1^2} \tag{15}$$

The clear statement of the above equations. The suspension damping coefficient is:

$$C = \frac{\rho A^3 \dot{x}}{C_1^2 A_1^2} \tag{16}$$

## 3. Suspension Model for 4 - DOF Half Car

**Figure 2** shows the four-degrees-of-freedom half-car model that was employed in this study. The model system comprised the sprung mass, the unsprung masses, the damping coefficient, and the wheel stiffness of the front part of the car, as well as the same parameters in the rear part of the car.

The system's four differential equations may be obtained from its four degrees of freedom. The differential equation corresponding to the sprung mass is influenced by the suspension as well as the sprung masses of the front and rear tires. The linear suspension system for a half-car, 4 DOF, is mathematically modeled. With the use of Newton's second law of motion, the equations of motion for each of the two moving masses are determined as shown in **Figure 2**. The equations of the linear passive suspension system are as follows:

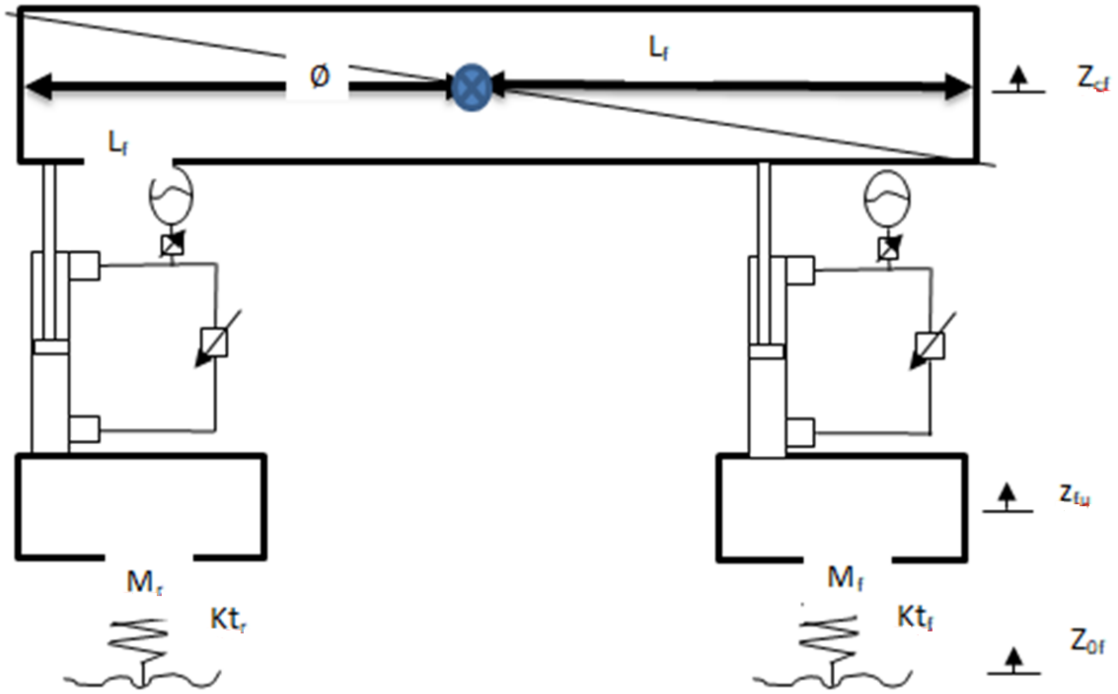


**Figure 2**. Half-vehicle model

$$M_B \ddot{Z}_c = F_{Hpf} + F_{Hpr} \quad (17)$$

$$I_{yy}\ddot{\emptyset} = -L_f F_{Hpf} + L_r F_{Hpr} \quad (18)$$

$$M_{uf}\ddot{Z_{fu}} = k_{tf}\left(z_{of} - Z_{uf}\right) - F_{Hpf} \quad (19)$$

$$M_{ur}\ddot{Z_{ru}} = k_{tr}(z_{or} - Z_{ur}) - F_{Hpr} \quad (20)$$

Where $(\ddot{\emptyset}, \dot{\emptyset}, \emptyset)$ are the angular acceleration, the angular velocity, and the angular displacement. $(\ddot{Z}_c, \dot{Z}_c, Z_c)$ are the acceleration, speed, and displacement of the floating mass. $(\ddot{Z_{ru}}, \dot{Z_{ru}}, Z_{ru})$ is the acceleration, speed, and displacement of the unsprung rear mass. $(\ddot{Z_{fu}}, \dot{Z_{fu}}, Z_{fu})$ is the unsprung front mass's acceleration, speed, and displacement. The lengths from CG to anterior and posterior are lf and lr, respectively.

Equations (17 and 18) can be derived from the floating mass, on the one hand, the vertical force analysis, and on the other hand the momentum analysis. First, let's look at the force analysis, to eliminate the denominator of the constant value obtained above, the spring constant is multiplied by the difference in vertical displacement, and the damper constant is multiplied by the difference in relative speed. At this moment, the displacement resulting from the distance between the center of gravity and the wheel is positive (+) for the front wheel and negative (-) for the rear wheel. According to the equilibrium of forces, the direction of lf (Ø) and lr (Ø) is opposite, since the rear wheel acts in the opposite z-direction. The second is an analysis of the moment (couple). In the case of the moment, it can be expressed as above, since it can be expressed as the product of force and distance. Since theta is very small in size, we approximate sin (Ø) to Ø. Equations (19 and 20) can be derived from each wheel.

## 4. Control Strategy of the Active Hydro-Pneumatic Model

Control methods have been employed to implement active and passive hydro-pneumatic suspensions. Land vehicles are also a very universal example because at least in industrialized countries, practically everyone has driven a car at some point. An automobile quarter model is also easily perceived as a system with several aims, some of which contradict one another [15]. Most studies focus on controlling the forces generated by struts and springs. Some studies have focused on changing the kinematic properties of a suspension system [14].

### *4.1. Approaches Based on LQR for Vehicle Suspension Control*

Linear Quadratic Regulator (LQR) is a control strategy commonly used in vehicle suspension systems. The LQR algorithm optimizes the control gains by minimizing the performance index J. The performance index J can be represented as follows [8]:

$$J = \int_0^{\infty} (x^T Qx + u^T Ru)\, dt \quad (21)$$

In this expression, x represents the vector of system states at time t, u represents the vector of control inputs at time t, and T denotes the transpose operation. Q is a positive semi definite matrix that weights the state deviations, and R is a positive definite matrix that weights the control effort.

### 4.2. H-Infinity Control for a Vehicle Suspension Control

H-infinity control is a robust control technique used in vehicle suspension systems to design controllers that can handle uncertainties and disturbances in the system dynamics. It aims to minimize the effect of disturbances on the system while achieving the desired performance objectives. **Figure 3** presented an H-infinity controller closed-loop.

### 4.3. PID Control for a Vehicle Suspension Control

The PID controller is the feedback controller. Its algorithm is discussed according to Eq. (22):

$$u(t) = K(e(t) + \frac{1}{T_i \int_0^t e(\tau)d\tau} + T_d de(t)/dt \quad (22)$$

Where,
y: The measured process variable,
u: control signal and e the control deviation
e= the error ($e = y_{sp} - y$)
K: proportional gain
$T_i$: Integral time
$T_d$: Derivative time

The error is the difference between the output signal $y_{sp}$ and the reference signal y. The P-term, I-term, and D-term are the three terms that make up the control signal. The PID algorithm is described by the transfer function [8]:

$$G(s) = K(1 + \frac{1}{sT_i} + \frac{sT_d}{\alpha sT_d} + 1) \quad (23)$$

## 5. Road Profile

ISO 8608 establishes a standardized framework for characterizing the roughness of roads and evaluating their impact on vehicle dynamics. These classifications help in evaluating the performance of vehicle suspension systems and designing control strategies to improve ride comfort and handling under various road conditions.

According to ISO 8608, the road is classified into eight distinct classes, each representing a specific type of road surface, roughness, and irregularities, from very smooth road surfaces (A) to unique road surfaces (H) [31]. The power spectral density (PSD) is a measure of statistics for analyzing the frequency content of road profiles. The PSD of the vertical road profile displacement $G_d$ is described in terms of angular spatial frequency $n$ as:

$$G_d(n) = G_d(n_o) * (\frac{n}{n_o})^{-w} \quad (24)$$

Where (w) signifies waviness and the undulation exponents (waviness index) are set between 1.8 and 3.3, w is set to 2 for the majority of the road surface at a constant velocity, and ($n_0$) is a reference angular spatial frequency equal to 1 rad/m [32]–[34].

Eq. (24) can produce a wide range of power spectrum densities. The ISO 8608 standard includes a classification of road roughness in terms of angular spatial frequency n predicted from a large number of measurements, as illustrated in **Table 1**.

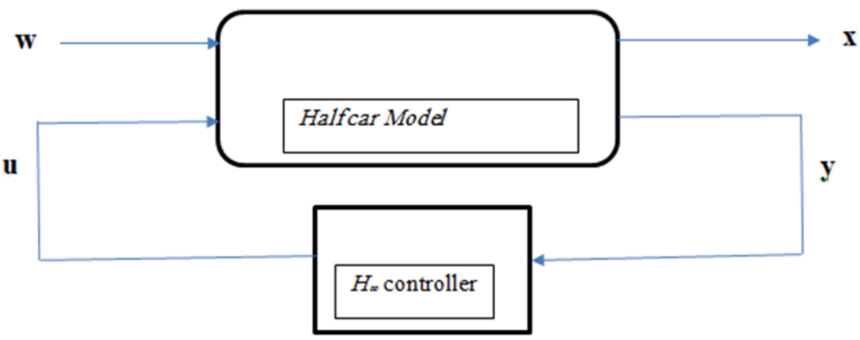


**Figure 3**. Active suspension system H-infinity controller

**Table 1**. ISO 8608 values of $G_d$ ($n_o$) [3]

| Road Class | $G_d$ ($n_o$) ($10^{-6}$ $m^3$) | |
|---|---|---|
| | **Lower value** | **Upper value** |
| Class (A) | ------ | 32 |
| Class (B) | 32 | 128 |
| Class (C) | 128 | 512 |
| Class (D) | 512 | 2048 |
| Class (E) | 2048 | 8192 |
| Class (F) | 8192 | 32768 |
| Class (G) | 32768 | 131072 |
| Class (H) | 131072 | --------- |

## 6. Results and Discussion

To manage the damping force of the suspension system, the 4-DOF half-car model's passive and active hydro-pneumatic suspensions were employed with different controller systems. Matlab/Simulation software was applied to conduct simulation for this work, with a simulation duration of 10 seconds. A simulation model is developed to assess the dynamic behavior of both the passive suspension system and the active suspension system in a half-car suspension setup, utilizing LQR, PID, and H-infinity control methods.

Body acceleration and displacement, front and rear acceleration and displacement, dynamic tire load at each wheel, as well as pitch acceleration and displacement according to each controller, are compared through simulation. The simulation results are presented in terms of root mean square (RMS) values both in the time and frequency domains. **Table 2**, lists the parameters of the vehicle in this model.

### 6.1. *Vehicle Body Acceleration (Vertical body Acceleration)*

**Figure 4**, shows the car body acceleration on a random road profile with hydro-pneumatic passive and active suspensions. The results of the validation between passive and active hydro-pneumatic suspensions with various controllers are presented, considering time and frequency domains, power spectral density, and root mean square values. **Figure 4**, shows the RSM values for the body acceleration. As seen, the RMS value under the H-infinity controller system is substantially decreased by about 50% compared to the RMS value under the passive system. The RMS value under the PID controller system is substantially decreased by about 26% compared to the RMS value under the passive system. This demonstrates how successful the H-infinity, PID, and LQR controllers are at absorbing vehicle vibration as compared to a passive system. Each control system greatly lessens body acceleration, ensuring a more comfortable ride.

### 6.2. *Pitch Acceleration (Body angular acceleration)*

The pitch acceleration of each passive and active hydro-pneumatic suspension under various control schemes is performed for comparison. The simulation results for the pitch acceleration for the passive and active hydro-pneumatic suspensions with different controllers are shown in **Figure 5**. When the simulation results for the different systems are compared, it is clear

**Table 2**. Half car model parameters

| Parameters | Value |
|---|---|
| Body mass, $M_B$ | 700 $Kg$ |
| Front unsprung mass, $M_{uf}$ | 40 $Kg$ |
| Rear unsprung mass$M_{ur}$ | 35.5 $Kg$ |
| Front suspension spring stiffness, $K_{sf}$ | 1990 $N/m$ |
| Front suspension spring stiffness, $K_{sf}$ | 17500 $N/m$ |
| Front tire spring stiffness, $K_{tf}$ | 175500 $N/m$ |
| Rear tire spring stiffness, $K_{tr}$ | 175500 $N/m$ |
| Distance from the front axle to C.G, $L_f$ | 2.3 $m$ |
| Distance from rear axle to C.G, $L_r$ | 2.3 $m$ |
| Wheel Base, $L$ | 4.6 $m$ |
| Body pitch moment of inertia, $I_{yy}$ | 2460 $Kg.m^2$ |

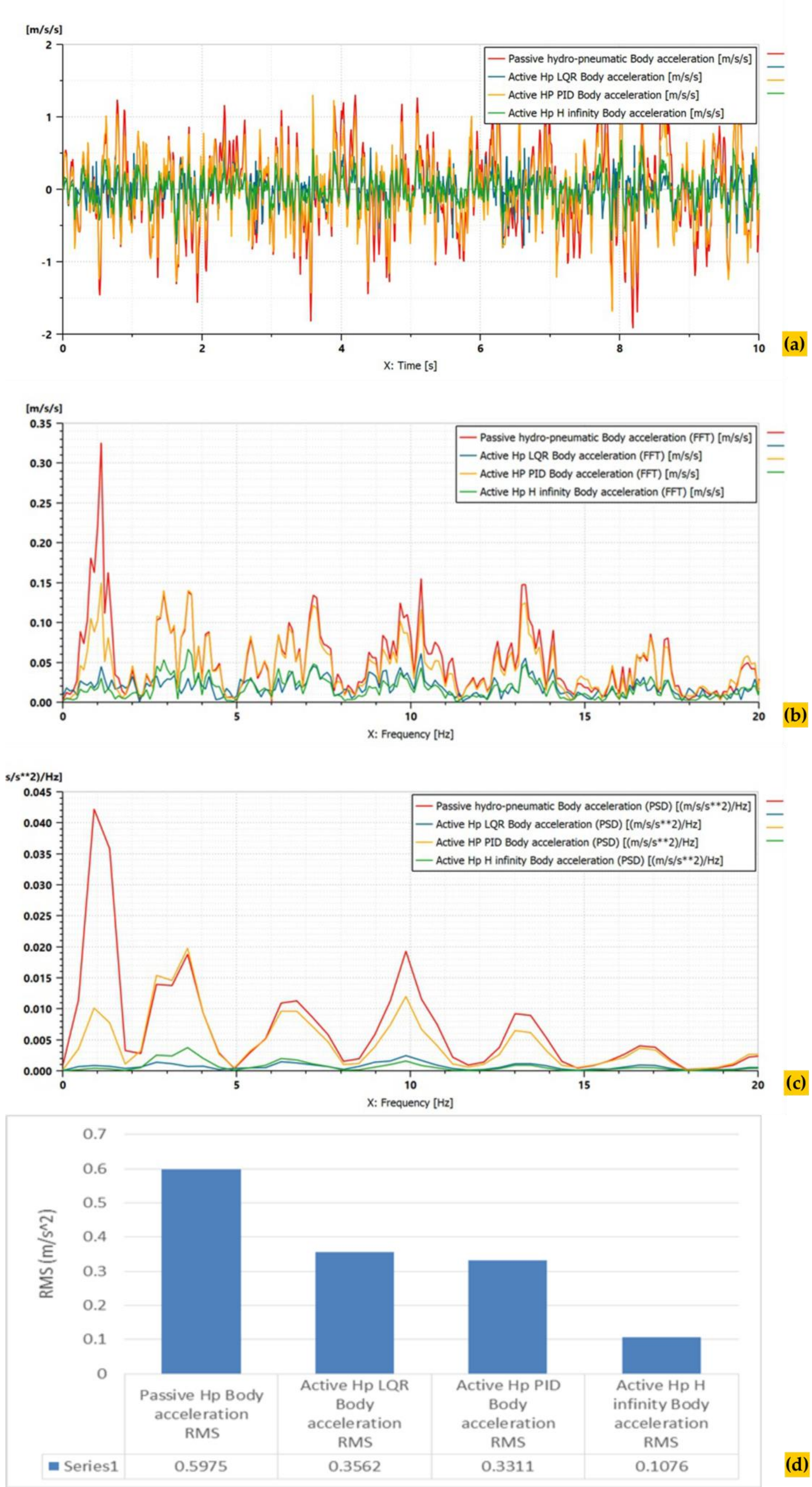


**Figure 4**. The passive, active LQR, PID, and H-infinity hydro-pneumatic suspension systems in terms of body acceleration with random road. (a) Time domain. (b) Frequency domain. (c) PSD (d) RMS.

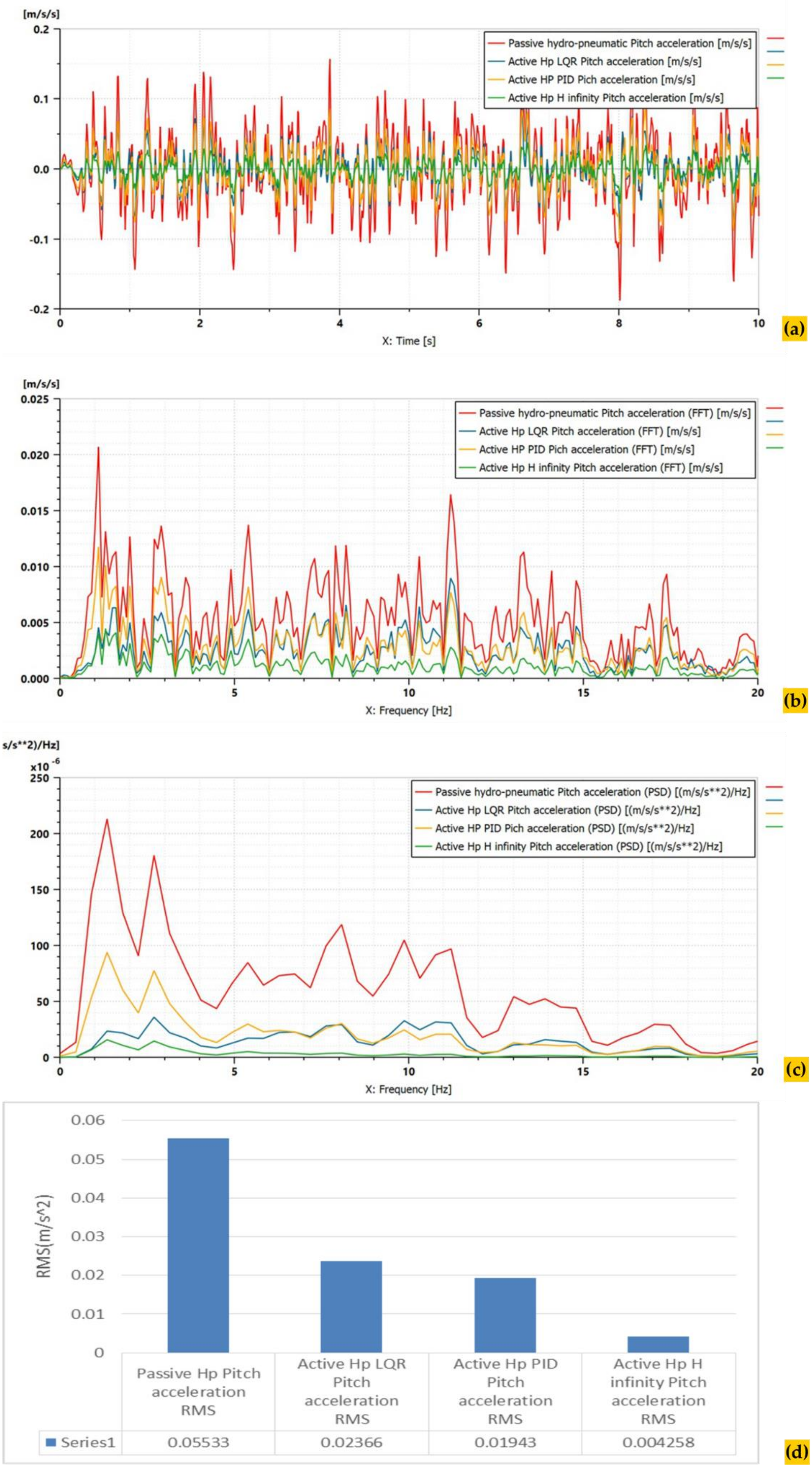


**Figure 5**. The passive, active LQR, PID, and H-infinity hydro-pneumatic suspension systems in terms of pitch acceleration with a random road. (a) Time domain. (b) Frequency domain. (c) PSD (d) RMS.

that active suspension with H-infinity control has a significant effect on pitch acceleration, with the presence of H-infinity control reducing pitch acceleration by around 92% in RMS when compared to passive hydro-pneumatic suspension. According to the figure, the PID control outperforms the LQR control in terms of pitch acceleration reduction. The PID control reduces pitch acceleration by around 65%, whereas the LQR control reduces pitch acceleration by about 57%.

### *6.3. Front / Rear Suspension Working Space (SWS)*

Figure 6 and Figure 7, show the change of the suspension working space (SWS) with passive hydro-pneumatic and active hydro-pneumatic with different types of control techniques in suspension systems for front and rear wheels, respectively. Suspension working space is a key design characteristic that is heavily influenced by spring stiffness and so impacts ride comfort. In actuality, the working space must be constrained by the vehicle's design and configuration.

Figure 6, depicts the suspension working space profile in both the time and frequency domains as a result of variations in the road profile of the front wheel. When using active suspension with H-infinity control, the maximum RMS value was 72% lower than when using a passive suspension system. Similarly, Figure 7 shows that the hybrid control offers the lowest displacement with reduced peaks when compared to passive suspension and semi-active LQR and PID control. The H-infinity control reduced the maximum RMS value of displacement by 72%, but the PID reduced the SWS by 50 % and 46% when compared to the passive.

### *6.4. Front / Rear Dynamic Tire Load (DTL)*

The comparison between different dynamic tire loads in the response frequency and time domains of passive, LQR, PID, and H-infinity for the front tires is presented in Figure 8. While Figure 9, depicts the same parameters for the rear tires. It may be seen that the dynamic tire load of both the front and rear wheels with active suspension with H-infinity control was found to be lower than that of passive and the other controller systems for most of the frequencies between 8 and 20 Hz, implying better handling compared with passive and active suspension with other controllers. According to the time domain results and RMS values of front wheel dynamic tire load under the passive suspension system and the active suspension with three control methods, the RMS value of dynamic tire load is reduced from 527 (N) in the passive suspension to 120 (N) when the active suspension with H-infinity control is used. The RMS value of the rear dynamic tire load is reduced from 493 (N) in the case of passive suspension to 112 (N) when an active suspension system with H-infinity control is used.

Table 3, shows the different types of hydro-pneumatic suspension controls and their RMS acceleration, displacement, and dynamic tire load values, which means that there is different ride comfort and handling for each type of control. It can be seen from the results that the H-infinity control has a lower RMS body acceleration and wheelbase value than the other control systems so more driving comfort is provided. Driving comfort and RMS acceleration value have an inversely proportionate relationship to one another. The dynamic RMS tire load values on both the front and rear wheels give a lower value when the H-infinity control strategy is used. Table 3, demonstrates that, as compared to the passive suspension, the dynamic tire load RMS improved by 77% and 76% by using the active hydro-pneumatic suspension based on hybrid control for the front and rear wheels, respectively.

Table 3. RMS values of the different suspension controllers.

| No | Type of control | Body Acc. | Pitch Acc. | Front SWS. | Rear SWS. | Front DTL. | Rear DTL |
|---|---|---|---|---|---|---|---|
| 1 | Passive | 0.5975 | 0.05533 | 0.01036 | 0.006219 | 493.4 | 537.2 |
| 2 | LQR | 0.3562 | 0.02366 | 0.005646 | 0.00328 | 154.4 | 170.6 |
| 3 | PID | 0.3311 | 0.01943 | 0.005193 | 0.003673 | 151.5 | 218.7 |
| 4 | H-infinity | 0.1076 | 0.004258 | 0.00291 | 0.002067 | 112.8 | 120.7 |

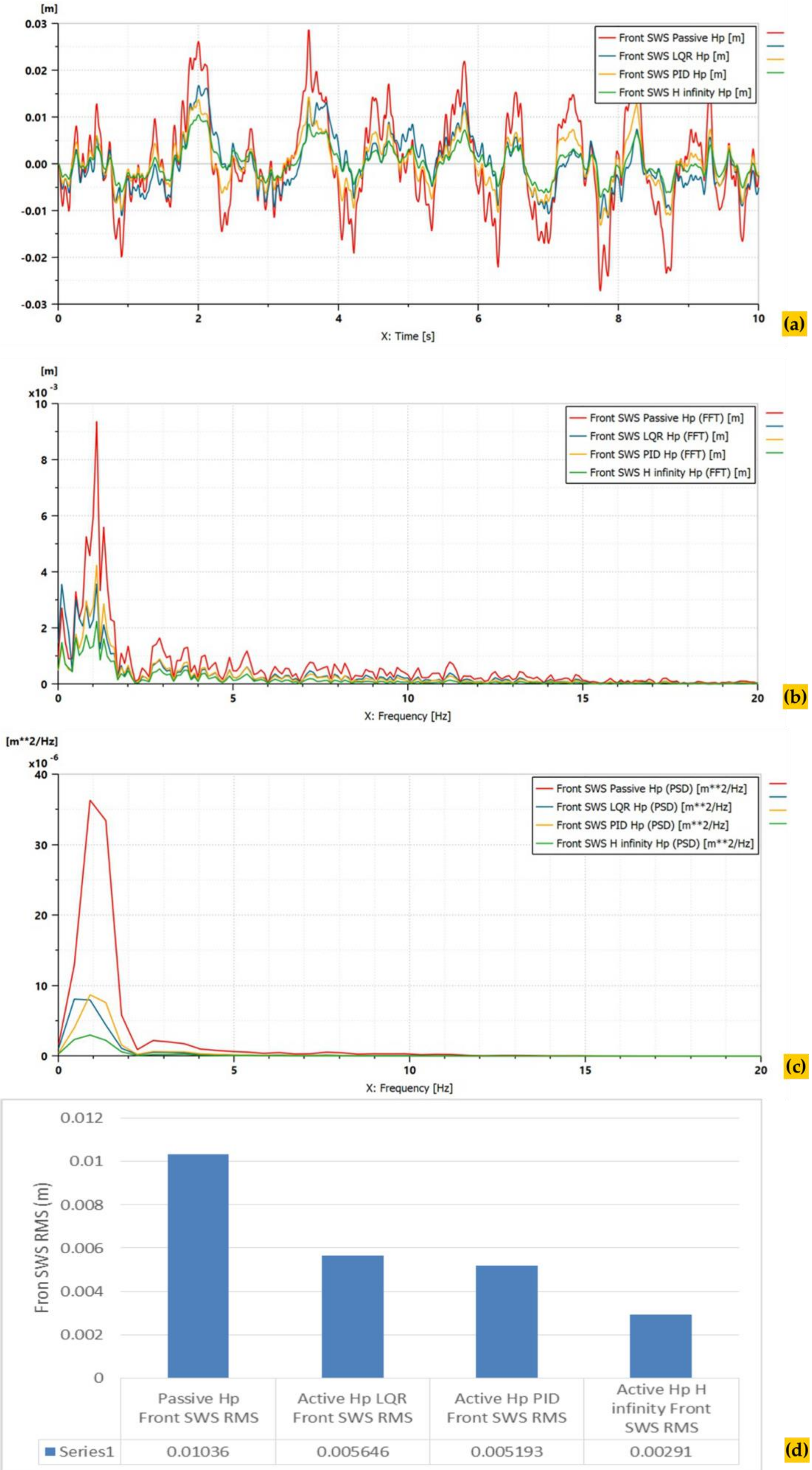


**Figure 6**. Comparison between the passive, active LQR, PID, and H-infinity hydro-pneumatic suspension systems in terms of suspension working space (SWS) with a random road for the front wheel. (a) Time domain. (b) Frequency domain. (c) PSD (d) RMS.

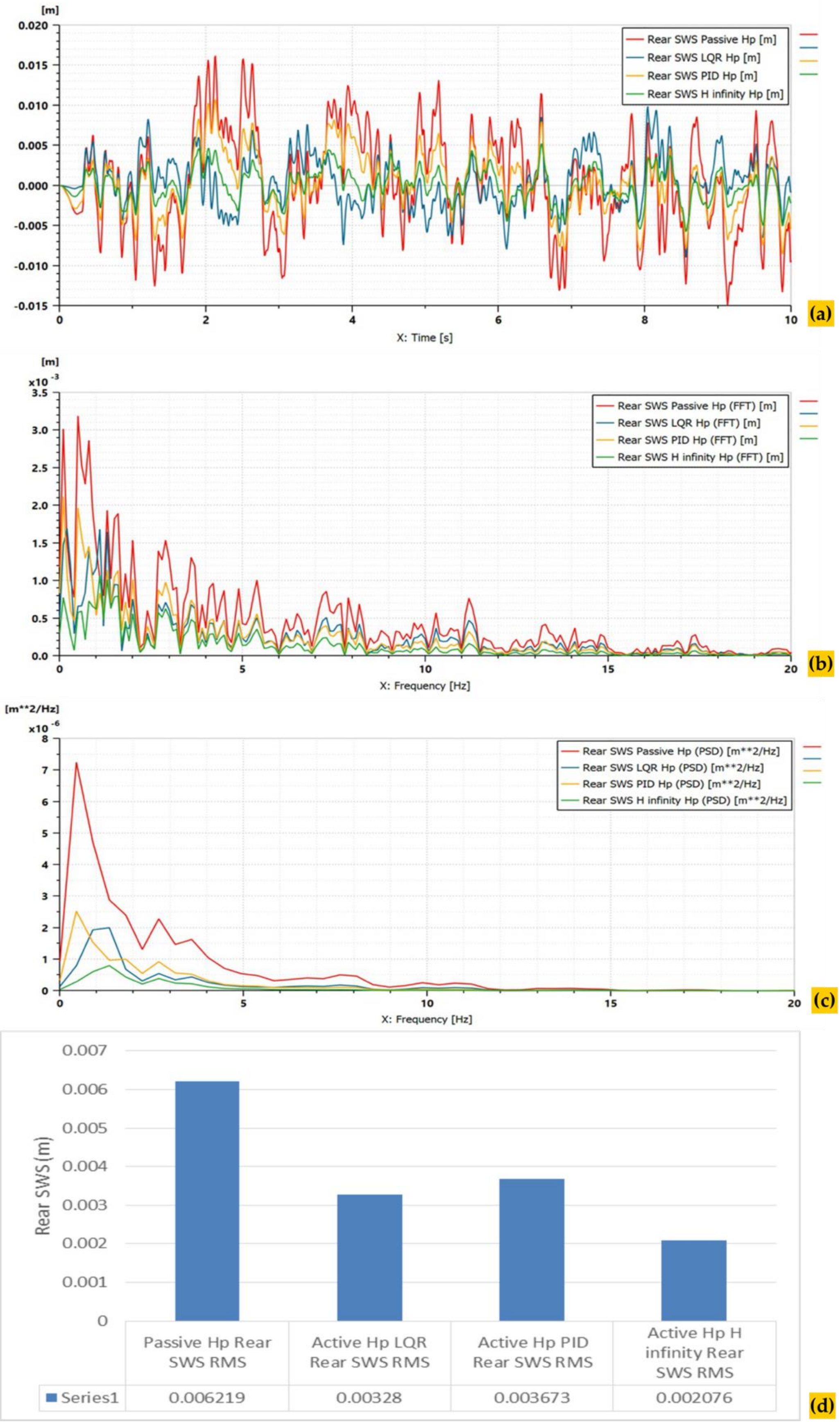


**Figure 7**. Comparison between the passive, active LQR, PID, and H-infinity hydro-pneumatic suspension systems in terms of suspension working space (SWS) with a random road for the rear wheel. (a) Time domain. (b) Frequency domain. (c) PSD (d) RMS.

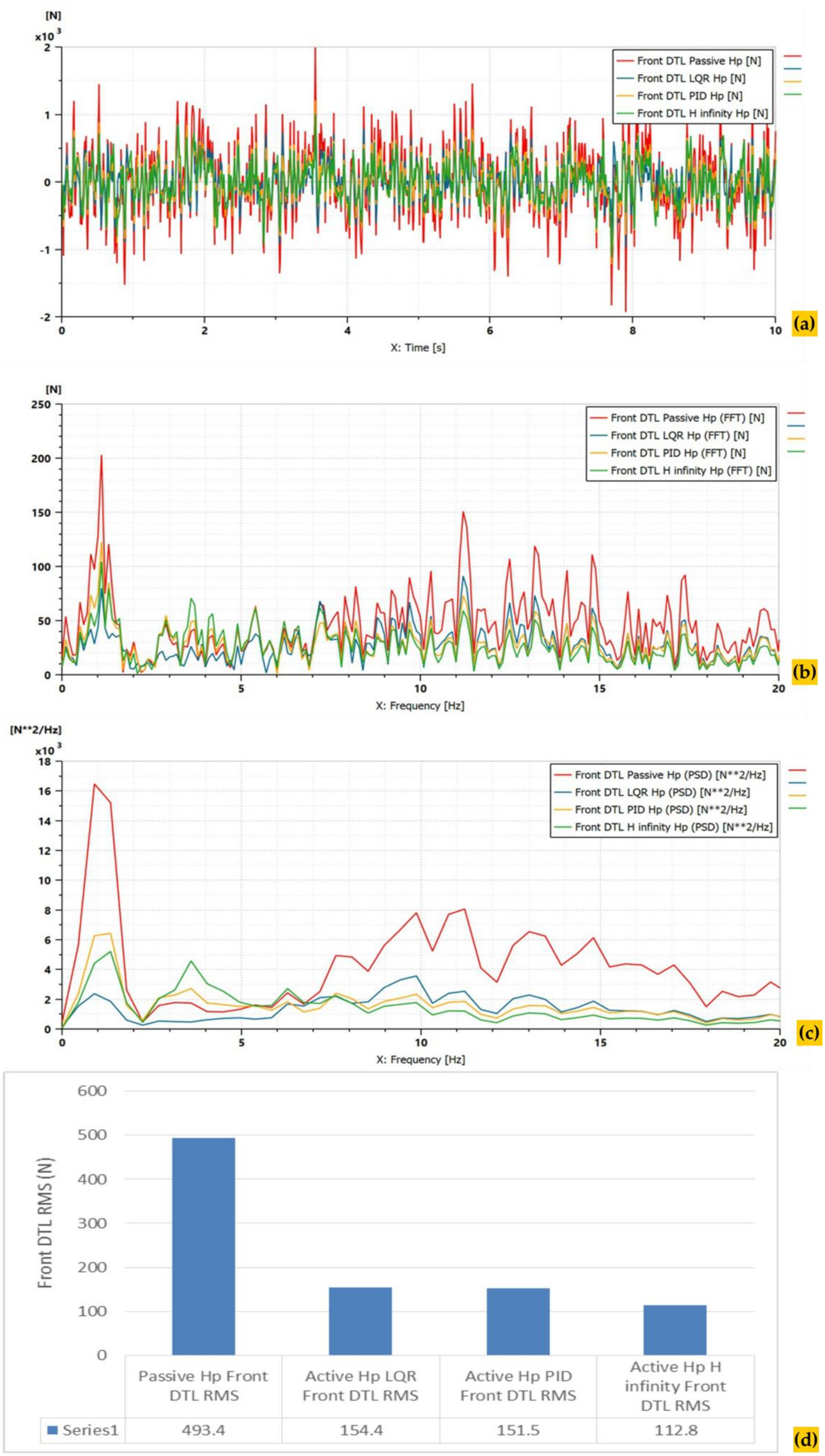


**Figure 8**. Comparison between the passive, LQR, PID, and H-infinity hydro-pneumatic active suspension systems in terms of dynamic tire load with random road for the front wheel. (a) Time domain. (b) Frequency domain. (c) PSD (d) RMS

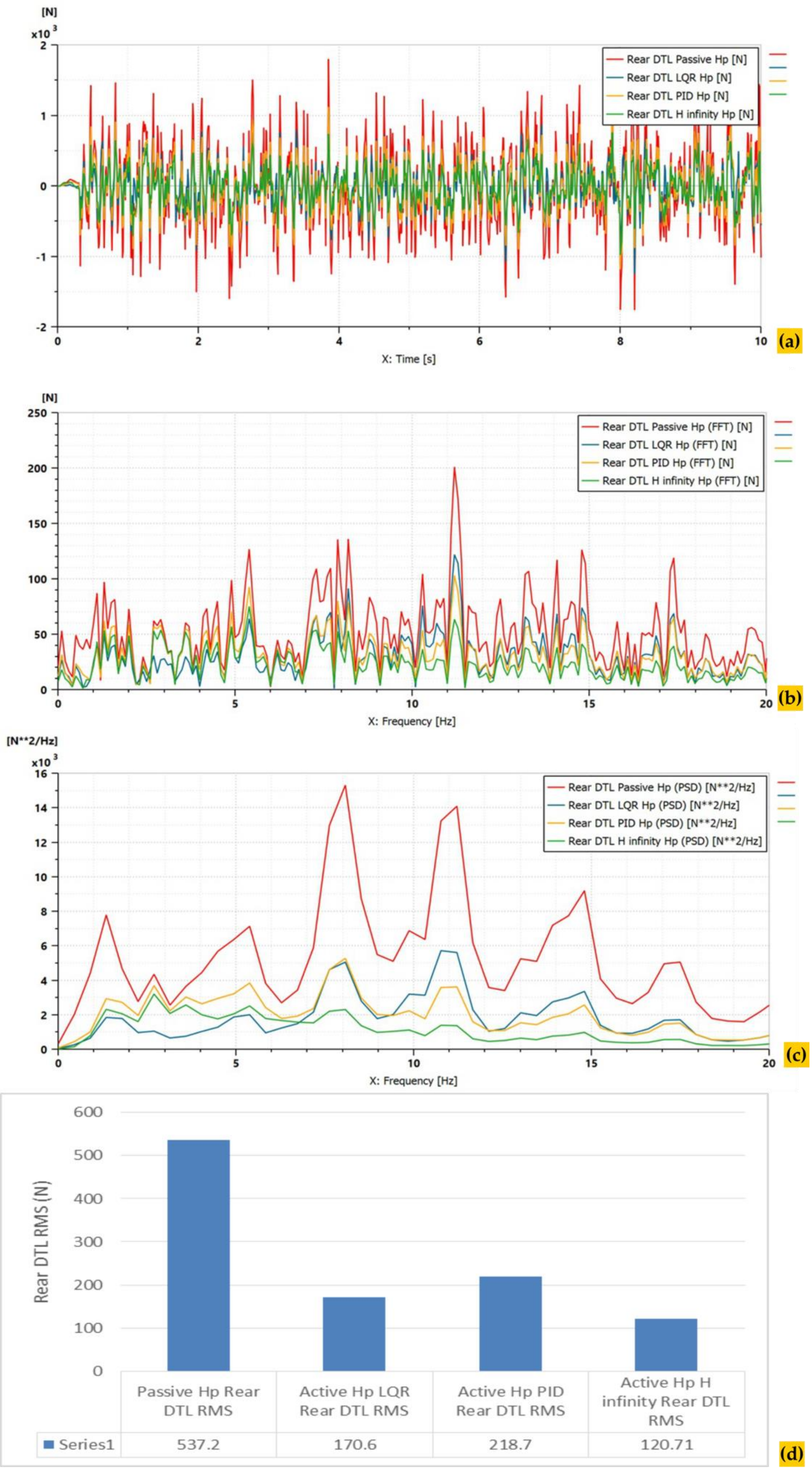


**Figure 9**. Comparison between the passive, LQR, PID, and H-infinity hydro-pneumatic active suspension systems in terms of dynamic tire load with random road for the rear wheel. (a) Time domain. (b) Frequency domain. (c) PSD. (d) RMS.

A higher DTL, however, denotes unfavorable conditions for maintaining the appropriate level of vehicle stability. Table 3, also includes the RMS values of the working space of the front and rear suspensions for passive and active suspension systems. These results demonstrate that the workspace of the front and rear suspensions with the hybrid control technique is much smaller than the working space with the other dynamic control systems. As a consequence, driving comfort may be enhanced without changing the working space of the suspension.

## 7. Conclusion

In summary, a controlled hydro-pneumatic suspension system with four degrees of freedom has been developed. The system employs three distinct control strategies, namely LQR, PID, and H-infinity control, to effectively regulate vertical vibrations. Through comprehensive evaluation using Matlab/Simulink and subjecting the system to random road excitation, the performance of the active suspension model has been compared to its passive suspension counterpart. The control strategies, which utilize body verticals, wheelbase acceleration, dynamic tire load, and suspension working space, have been thoroughly examined. The H-infinity-controlled active suspension system has demonstrated significant enhancements, achieving an 81% improvement in body acceleration and a 92% improvement in pitch acceleration compared to the passive hydro-pneumatic suspension. Similarly, the LQR-controlled suspension exhibited a 40% and 57% enhancement in body and step acceleration, respectively, compared to the passive counterpart. The PID-controlled suspension yielded improvements of 64% and 44% in step acceleration and body acceleration, respectively, over the passive hydro-pneumatic suspension. Furthermore, the H-infinity control strategy notably expanded the working space of the front and rear suspensions by 72% and 67%, respectively, compared to the passive suspension. The LQR-controlled suspension improved the working space of the front and rear suspensions by 46% and 47%, respectively, relative to the passive suspension. The PID-controlled suspension demonstrated a significant improvement in the working space of both the front and rear suspensions, with a 50% increase in the front suspension and a 41% increase in the rear suspension compared to the passive suspension. These results showed that the active suspension system with the new damper, particularly when employing H-infinity and LQR control strategies, reduced the vertical vibrations and enhancing the overall performance of the suspension system and therefore the stability of the vehicle specially during cornering.

## Author's Declaration

### Authors' contributions and responsibilities

The authors made substantial contributions to the conception and design of the study. The authors took responsibility for data analysis, interpretation and discussion of results. The authors read and approved the final manuscript.


### Funding

No funding information from the authors.


### Availability of data and materials

All data are available from the authors.

### Competing interests

The authors declare no competing interest.

### Additional information

No additional information from the authors.

## References


[1] R. Alkhatib, G. Nakhaie Jazar, and M. . Golnaraghi, "Optimal design of passive linear suspension using genetic algorithm," *Journal of Sound and Vibration*, vol. 275, no. 3–5, pp. 665–691, Aug. 2004, doi: 10.1016/j.jsv.2003.07.007.

[2] T. Abut and E. Salkim, "Control of Quarter-Car Active Suspension System Based on Optimized Fuzzy Linear Quadratic Regulator Control Method," *Applied Sciences*, vol. 13, no. 15, p. 8802, Jul. 2023, doi: 10.3390/app13158802.

[3] L. Yang, R. Wang, X. Meng, Z. Sun, W. Liu, and Y. Wang, "Performance analysis of a new hydropneumatic inerter-based suspension system with semi-active control effect," *Proceedings of the Institution of Mechanical Engineers, Part D: Journal of Automobile Engineering*, vol. 234, no. 7, pp. 1883–1896, Jun. 2020, doi: 10.1177/0954407019894189.

[4] N. M. Ghazaly and A. O. Moaaz, "Hydro-Pneumatic Passive Suspension System

Performance Analysis using AMESim Software," *International Journal of Vehicle Structures and Systems*, vol. 12, no. 1, Jun. 2020, doi: 10.4273/ijvss.12.1.02.

[5] I. Dridi, A. Hamza, and N. Ben Yahia, "Control of an active suspension system based on long short-term memory (LSTM) learning," *Advances in Mechanical Engineering*, vol. 15, no. 2, p. 168781322311567, Feb. 2023, doi: 10.1177/16878132231156789.

[6] F. Jeniš, M. Kubík, T. Michálek, Z. Strecker, J. Žáček, and I. Mazůrek, "Effect of the Magnetorheological Damper Dynamic Behaviour on the Rail Vehicle Comfort: Hardware-in-the-Loop Simulation," *Actuators*, vol. 12, no. 2, p. 47, Jan. 2023, doi: 10.3390/act12020047.

[7] J. Theunissen, A. Tota, P. Gruber, M. Dhaens, and A. Sorniotti, "Preview-based techniques for vehicle suspension control: a state-of-the-art review," *Annual Reviews in Control*, vol. 51, pp. 206–235, 2021, doi: 10.1016/j.arcontrol.2021.03.010.

[8] T. A. Nguyen, "Advance the stability of the vehicle by using the pneumatic suspension system integrated with the hydraulic actuator," *Latin American Journal of Solids and Structures*, vol. 18, no. 7, 2021, doi: 10.1590/1679-78256621.

[9] F. Scheibe and M. C. Smith, "Analytical solutions for optimal ride comfort and tyre grip for passive vehicle suspensions," *Vehicle System Dynamics*, vol. 47, no. 10, pp. 1229–1252, Oct. 2009, doi: 10.1080/00423110802588323.

[10] N. Zhang, S. Yang, G. Wu, H. Ding, Z. Zhang, and K. Guo, "Fast Distributed Model Predictive Control Method for Active Suspension Systems," *Sensors*, vol. 23, no. 6, p. 3357, Mar. 2023, doi: 10.3390/s23063357.

[11] M. A. Karkoub and M. Zribi, "Active/semi-active suspension control using magnetorheological actuators," *International Journal of Systems Science*, vol. 37, no. 1, pp. 35–44, Jan. 2006, doi: 10.1080/00207720500436344.

[12] Y. Ko, K. Park, I. Baek, G. Kim, and J. Lee, "Study on Development of Virtual Components for Active Air Suspension System Based on HILS for Commercial Vehicle," *Transactions of the Korean Society of Automotive Engineers*, vol. 21, no. 2, pp. 26–36, Mar. 2013, doi: 10.7467/KSAE.2013.21.2.026.

[13] Q. Fu, J. Wu, C. Yu, T. Feng, N. Zhang, and J. Zhang, "Linear Quadratic Optimal Control with the Finite State for Suspension System," *Machines*, vol. 11, no. 2, p. 127, Jan. 2023, doi: 10.3390/machines11020127.

[14] A. O. Moaaz, A. S. Ali, N. M. Ghazaly, and M. M. Makrahy, "Performance Evaluation of Semi-Active Suspension for Passenger Vehicle through Skyhook, Groundhook and Hybrid Control Strategies," *International Journal of Vehicle Structures and Systems*, vol. 14, no. 5, Dec. 2022, doi: 10.4273/ijvss.14.5.04.

[15] A. Soliman and M. Kaldas, "Semi-active suspension systems from research to mass-market – A review," *Journal of Low Frequency Noise, Vibration and Active Control*, vol. 40, no. 2, pp. 1005–1023, Jun. 2021, doi: 10.1177/1461348419876392.

[16] Y. Zhang, T. Schauer, and A. Bleicher, "Optimized passive/semi-active vibration control using distributed-multiple tuned facade damping system in tall buildings," *Journal of Building Engineering*, vol. 52, p. 104416, Jul. 2022, doi: 10.1016/j.jobe.2022.104416.

[17] X. Ding, R. Li, Y. Cheng, Q. Liu, and J. Liu, "Design of and Research into a Multiple-Fuzzy PID Suspension Control System Based on Road Recognition," *Processes*, vol. 9, no. 12, p. 2190, Dec. 2021, doi: 10.3390/pr9122190.

[18] T. Nakayama, M. Morita, H. Kamimae, A. Nishihara, and K. Tuda, "Development of semi-active control system with PUDLIS," in *Proceedings of International Symposium on Advanced Vehicle Control (AVEC)*, 1996, no. 1, pp. 233–239.

[19] S. B. A. Kashem, K. B. Mustapha, and T. S. Kannan, "A study and review on vehicle suspension system and introduction of a high-bandwidth configured quarter car suspension system," *Australian Journal of Basic and Applied Sciences*, vol. 9, no. 30, pp. 59–66, 2015.

[20] S. Nagamatsu and T. Shiraishi, "A simple and novel control strategy for semi-active vibration suppression by a magnetorheological damper," *Journal of*

*Intelligent Material Systems and Structures*, vol. 33, no. 6, pp. 811–821, Apr. 2022, doi: 10.1177/1045389X211032288.

[21] A. Čerškus, V. Ušinskis, N. Šešok, I. Iljin, and V. Bučinskas, "Optimization of Damping in a Semi-Active Car Suspension System with Various Locations of Masses," *Applied Sciences*, vol. 13, no. 9, p. 5371, Apr. 2023, doi: 10.3390/app13095371.

[22] S. Kimbrough, "Bilinear modeling and regulator of variable component suspensions," *ASME WAM, AMD*, vol. 80, no. 4, 1986.

[23] H. E. Tseng, K. Yi, and J. K. Hedrick, "A comparison of alternative semi-active control laws," in *ASME WAM*, 1991, pp. 1–6.

[24] M. Valásek and M. Novák, "A new concept of semi-active control of truck's suspension," in *Proceedings of International Symposium on Advanced Vehicle Control*, pp. 141–151.

[25] M. Valášek, M. Novák, Z. Šika, and O. Vaculín, "Extended Ground-Hook - New Concept of Semi-Active Control of Truck's Suspension," *Vehicle System Dynamics*, vol. 27, no. 5–6, pp. 289–303, Jun. 1997, doi: 10.1080/00423119708969333.

[26] D. Hennecke and F. J. Zieglmeier, "Frequency dependent variable suspension damping—theoretical background and practical success," *Proceeding of Institution of Mechanical Engineers*, pp. 101–111, 1988.

[27] A. Ranjan, S. Prasanth, F. Cherian, J. P. Bhasker, and K. Ravi, "Adaptive hybrid control strategy for semi-active suspension system," *IOP Conference Series: Materials Science and Engineering*, vol. 263, p. 062062, Nov. 2017, doi: 10.1088/1757-899X/263/6/062062.

[28] F. D. Goncalves and M. Ahmadian, "A Hybrid Control Policy for Semi-Active Vehicle Suspensions," *Shock and Vibration*, vol. 10, no. 1, pp. 59–69, 2003, doi: 10.1155/2003/897173.

[29] S. Han, Z. Chao, and X. Liu, "A Semiactive and Adaptive Hybrid Control System for a Tracked Vehicle Hydropneumatic Suspension Based on Disturbance Identification," *Shock and Vibration*, vol. 2017, pp. 1–12, 2017, doi: 10.1155/2017/2741786.

[30] P. S. Els and B. Grobbelaar, "Investigation of the time-and temperature dependency of hydro-pneumatic suspension systems," SAE Technical Paper, 1993.

[31] P. Zheng and J. Gao, "Damping force and energy recovery analysis of regenerative hydraulic electric suspension system under road excitation: modelling and numerical simulation," *Mathematical Biosciences and Engineering*, vol. 16, no. 6, pp. 6298–6318, 2019, doi: 10.3934/mbe.2019314.

[32] A. O. Moaaz and N. M. Ghazaly, "Fuzzy and PID controlled active suspension system and passive suspension system comparison," *International journal of advanced science and Technology*, vol. 28, no. 16, pp. 1721–1729, 2019.

[33] A. Strydom and P. S. Els, "The Applicability of Hybrid Control to a Small Off-Road Vehicle Without a Differential," Aug. 2014, doi: 10.1115/DETC2014-34344.

[34] A. Gupta, N. Bharadwaj, S. Upadhyaya, and S. Upadhyaya, "Development of hybrid control algorithm for improvement of performance of Semi-Active Suspension System," *World Journal of Modelling and Simulation*, vol. 15, pp. 53–63, 2018.